ELSEVIER

Mechatronics 14 (2004) 701–714

MECHATRONICS

Combined PID and adaptive nonlinear control for servo mechanical systems

K.Z. Tang *, S.N. Huang, K.K. Tan, T.H. Lee

Department of Electrical and Computer Engineering, National University of Singapore, 4, Engineering Drive 3, Singapore 117576, Singapore

Abstract

This paper presents a robust control method for servo mechanical systems, based on a mixed PID/adaptive algorithm. A second-order linear dominant model is considered with an unmodeled part of dynamics that is possibly nonlinear and time-varying. The PID part of the controller is designed to stabilize the dominant model. The adaptive part of the controller is used to compensate for the deviation of the system characteristics from the dominant linear model to achieve performance enhancement. The advantage of the proposed controller is that it can cope with strong nonlinearities in the system while still using the PID control structure which is well known to many control engineers. The proposed control scheme guarantees the boundedness of the system states and parameter estimation.

Keywords: Adaptive nonlinear control; Servo mechanical systems

1. Introduction

The PID controller has remained, by far, as the most commonly used controller in practically all industrial control applications. The reason is that it has a simple structure which is easy to be understood by the engineers. Over the years, many techniques have been suggested for tuning of the PID parameters, such as the refined Ziegler–Nichols method [1], the gain-phase margin method [2], an optimization method [3], and one based on the *Internal Model Control* [4]. Among them, the

* Corresponding author. Fax: +65-6777-3117.
E-mail address: eletkz@nus.edu.sg (K.Z. Tang).

0957-4158/$ - see front matter
doi:10.1016/j.mechatronics.2004.01.007

model-based tuning methods appear to be very encouraging [5]. However, the limitations of PID control rapidly become evident when applied to more complicated systems such as those with a time-delay, poorly damped, nonlinear and time-varying dynamics. For these processes, nonlinear adaptive control may be necessary to achieve good control performance. Recently, a nonlinear PD control scheme has been developed for a robot tracking application [6]. Based on a first-order model, a nonlinear PI control has also been proposed by Huang et al. [7].

This paper presents a new combined PID and adaptive control scheme for a class of nonlinear servo mechanical system. In the proposed approach, a second-order model with an unknown nonlinear term that is nonlinear and time-varying is used as the dominant model of a class of nonlinear systems. PID control is applied to stabilize the nominal system based on this dominant model. The system nonlinearity is compensated using an adaptive scheme employing the radial basis function neural network (RBFNN). The stability and tracking performance associated with the scheme is regional in system states. Simulation and experimental results are provided to illustrate the effectiveness of the proposed control scheme.

2. Robust nonlinear PID control

In this section, the development of the proposed control scheme will be described systematically in details.

2.1. Problem formulation

The dynamics of a servo mechanical system can be described using a nonlinear mathematical model:

$$u(t) = K_e\dot{x} + Ri(t) + L\,\mathrm{d}i(t)/\mathrm{d}t, \tag{1}$$

$$f(t) = K_f i(t), \tag{2}$$

$$f(t) = m\ddot{x}(t) + \bar{f}_{\mathrm{fric}}(\dot{x}) + \bar{f}_{\mathrm{load}}(t), \tag{3}$$

where $u(t)$ and $i(t)$ are the time-varying motor terminal voltage and armature current respectively; $x(t)$ is the motor position; $f(t)$ and $\bar{f}_{\mathrm{load}}$ are the developed force and the applied load force respectively. $\bar{f}_{\mathrm{fric}}$ denotes the frictional force present. The physical significance of the other physical parameters are elaborated in [8].

Since the electrical time constant is much smaller than the mechanical one, the delay of electrical response can be ignored. With this simplification, the following equation can be obtained (see [9]):

$$\ddot{x} = \left(-\frac{K_f K_e}{R}\dot{x} + \frac{K_f}{R}u(t) - \bar{f}_{\mathrm{fric}} - \bar{f}_{\mathrm{load}} \right) \Big/ m. \tag{4}$$

Let

$$a = -\frac{K_f K_e}{mR}, \tag{5}$$

$$b = \frac{K_f}{mR}, \tag{6}$$

$$f_{\text{fric}} = \frac{1}{m}\bar{f}_{\text{fric}}, \tag{7}$$

$$f_{\text{load}} = \frac{1}{m}\bar{f}_{\text{load}}. \tag{8}$$

Thus, we have the following equivalent model:

$$\ddot{x} = a\dot{x} + bu - f_{\text{fric}} - f_{\text{load}}. \tag{9}$$

The frictional force affecting the movement of the translator can be modeled as a combination of Coulomb and viscous friction [10] as:

$$f_{\text{fric}} = [f_c + f_v|\dot{x}|]\text{sgn}(\dot{x}) + \delta f_{\text{fric}}, \tag{10}$$

where f_c is the minimum level of Coulomb friction and f_v is associated with the viscosity constant. δf_{fric} denotes possible directional bias associated with the Coulomb friction. For loading effects which are independent of the direction of motion, f_{load} can be described as:

$$f_{\text{load}} = f_l\text{sgn}(\dot{x}) + \delta f_{\text{load}}, \tag{11}$$

where δf_{load} denotes possible directional bias associated with the load which is the case when the load is transported in a direction aligned with gravitational force. Cumulatively, the frictional and load force can be described as one external disturbance F, given by:

$$F = [f_1 + f_2|\dot{x}|]\text{sgn}(\dot{x}) + \delta f, \tag{12}$$

where $f_1 = f_l + f_c$, $f_2 = f_v$ and $\delta f = \delta f_{\text{fric}} + \delta f_{\text{load}}$. Fig. 1 graphically illustrates the characteristics of F.

Define the tracking error $e(t) = x_d(t) - x(t)$ and write (9) as

$$\ddot{e} = a\dot{e} - bu + f_{\text{fric}} + f_{\text{load}} + \ddot{x}_d - a\dot{x}_d. \tag{13}$$

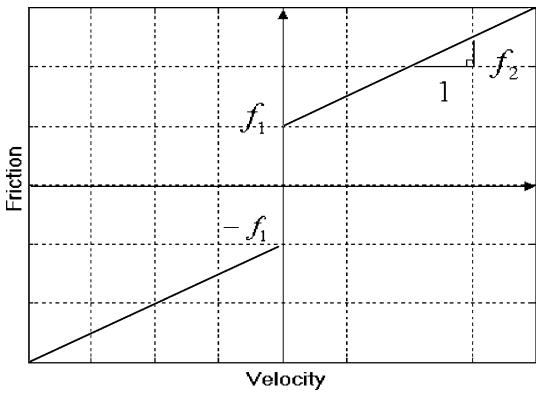

Fig. 1. F–$\dot{x}$ characteristics.

Let $d = -(f_{\text{load}} + \ddot{x}_d - a\dot{x}_d)/b$ and $f(x,\dot{x}) = -(f_{\text{fric}} + f_{\text{ripple}})/b$ and we have

$$\ddot{e} = a\dot{e} - bu - b[f(x,\dot{x}) + d]. \tag{14}$$

Assumption 2.1. It is assumed that the desired trajectories $x_d, \dot{x}_d, \ddot{x}_d$ are bounded. Thus, we can conclude that d is bounded, i.e.,

$$|d| < d_M, \tag{15}$$

since d_M is bounded.

Since $\frac{\mathrm{d}}{\mathrm{d}t}\int_0^t e(\tau)\,\mathrm{d}\tau = e$, let the system's variables be $z = [\int_0^t e(\tau)\,\mathrm{d}\tau\, e\dot{e}]^{\mathrm{T}}$. Then, (14) can be put into the following equivalent state equation:

$$\ddot{z} = Az + Bu + B[f(x,\ddot{x}) + d], \tag{16}$$

$$A = \begin{bmatrix} 0 & 1 & 0 \\ 0 & 0 & 1 \\ 0 & 0 & a \end{bmatrix}, \qquad B = \begin{bmatrix} 0 \\ 0 \\ -b \end{bmatrix}. \tag{17}$$

For the nominal system

$$\dot{z} = Az + Bu, \tag{18}$$

we propose the nominal control law $u_{\text{nom}} = Kz$ which is the standard PID control to guarantee uniform stability for the nominal system.

However, in order to compensate the effects of $f(x,\dot{x})$ which may possibly induce instability problems, it is possible to augment the nominal control signal with an additional signal to cancel the nonlinear terms. To this end, the RBFNN may be used to model $f(x,\dot{x})$. An additional control signal is thus provided by the RBFNN to compensate for the effects of $f(x,\dot{x})$. The main property of a RBFNN used here for estimation purposes is the function approximation property [11–13].

Since $f(x,\dot{x})$ is a nonlinear smooth function (unknown), it may be represented by a RBFNN with constant 'ideal' weights w_i, $i = 0, 1, 2, \ldots, m$ and a sufficient number of basis functions $\phi(\cdot)$ on the compact set $\Omega = \{X | \|X_d - X\| \leqslant M\}$ where $X_d = [x_d, \dot{x}_d]^{\mathrm{T}}$. Thus,

$$f(x,\dot{x}) = \sum_{i=0}^{m} w_i \phi_i(c_i X) + \epsilon, \tag{19}$$

where ϵ is the RBFNN approximation error satisfying $|\epsilon| \leqslant \epsilon_M$ with constant ϵ_M and $\phi_i(c_i X)$ is given by

$$\phi_i(c_i X) = \exp\left(-\frac{\|X - c_i\|^2}{2\sigma_i^2}\right), \tag{20}$$

where c_i is a two-dimensional vector representing the center of the ith basis function, and σ_j is the variance representing the spread of the basis function. In general, the RBF basis parameters c_i and ideal RBF weights w_i^* are unknown and need to be

estimated in the control design. Note that the set Ω and the bounding constant ϵ_M can be arbitrarily large.

$$f(x,\dot{x}) = W^{\mathrm{T}}\Phi(C^{\mathrm{T}}\overline{X}) + \epsilon, \tag{21}$$

where $W = [w_0, w_1, \ldots, w_m]^{\mathrm{T}}$, $\Phi = [\phi_0, \phi_1, \ldots, \phi_m]^{\mathrm{T}}$, $\overline{X} = [X^{\mathrm{T}}, 1]^{\mathrm{T}}$.

Let $\widehat{W}$, $\widehat{C}$ be estimates of the ideal W and C. Define the estimation errors as

$$\widetilde{W} = W - \widehat{W}, \qquad \widetilde{C} = C - \widehat{C}. \tag{22}$$

Then, applying the same approach of [14,15], we can obtain:

$$\widetilde{\Phi} = \Phi - \widehat{\Phi} = \Phi(C^{\mathrm{T}}\overline{X}) - \Phi(\widehat{C}\overline{X}). \tag{23}$$

The Taylor series expansion for a given $\overline{X}$ may be written as:

$$\Phi(C^{\mathrm{T}}\overline{X}) = \Phi(\widehat{C}^{\mathrm{T}}\overline{X}) + \Phi'(\widehat{C}^{\mathrm{T}}\overline{X})\widetilde{C}^{\mathrm{T}}\overline{X} + \mathrm{O}(\widetilde{C}^{\mathrm{T}}\overline{X})^2. \tag{24}$$

Then

$$\begin{aligned} W^{\mathrm{T}}\Phi(C^{\mathrm{T}}\overline{X}) - \widehat{W}^{\mathrm{T}}\Phi(\widehat{C}\overline{X}) = {} & \widetilde{W}^{\mathrm{T}}[\Phi(\widehat{C}^{\mathrm{T}}\overline{X}) - \Phi'(\widehat{C}^{\mathrm{T}}\overline{X})\widehat{C}^{\mathrm{T}}\overline{X}] \\ & + \widehat{W}^{\mathrm{T}}\Phi'(\widehat{C}^{\mathrm{T}}\overline{X})\widetilde{C}^{\mathrm{T}}\overline{X} + d_u, \end{aligned} \tag{25}$$

where

$$d_u = \widetilde{W}^{\mathrm{T}}\Phi'(\widehat{C}^{\mathrm{T}}\overline{X})C^{\mathrm{T}}\overline{X} + W^{\mathrm{T}}O(\widetilde{C}^{\mathrm{T}}\overline{X})^2. \tag{26}$$

Since Φ is the RBF function, every element of $\Phi(C^{\mathrm{T}}\overline{X}) - \Phi(\widehat{C}^{\mathrm{T}}\overline{X})$ is bounded by $2M$. Thus, we have

$$|d_u| \leqslant \|C\|_F\|\overline{X}\widehat{W}^{\mathrm{T}}\Phi'(\widehat{C}^{\mathrm{T}}\overline{X})\|_F + \|W\|\|\Phi'(\widehat{C}^{\mathrm{T}}\overline{X})\widehat{C}^{\mathrm{T}}\overline{X}\| + 2M|W|_1. \tag{27}$$

2.2. Combined PID and adaptive control

In this subsection, we propose a combined control law constituting PID control and an adaptive control (provided by the RBFNN). The control structure is as shown in Fig. 2. We will show that the nominal system can be made asymptotically stable by properly choosing the PID parameters while the uncertain term can be compensated by the RBFNN. Thus, considering the system (16), the control input is given by

$$u = Kz - \hat{f}(x,\dot{x}) - \mathrm{sgn}(z^{\mathrm{T}}PB)\hat{d}, \tag{28}$$

where Kz is standard PID control and $\hat{f}(x,\dot{x})$ is the RBF functional estimate of $f(x,\dot{x})$ given by

$$\hat{f}(x,\dot{x}) = \sum_{i=0}^{m}\hat{w}_i\phi_i(x,\dot{x}), \tag{29}$$

where $\hat{w}_i$ is the estimate of the ideal weighting w_i^*, and $\mathrm{sgn}(z^{\mathrm{T}}PB)\hat{d}$ is a robustification term which provides robustness in the face of bounded disturbances.

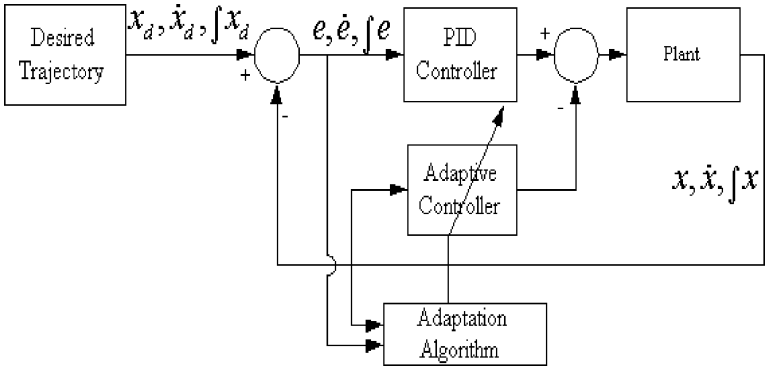

Fig. 2. Control structure.

For PID control, much work has been done in this area. In principle, we can employ the existing PID tuning methods such as the gain and phase margin method, dominant pole method [16], and etc. Since we can design the PID controller to ensure nominal stability for the dominant model, the following Lyapunov equation holds:

$$(A + BK)^{\mathrm{T}}P + P(A + BK) = -I. \tag{30}$$

Let $\overline{A} = A + BK$. The following controller is proposed

$$u = Kz - \widehat{W}^{\mathrm{T}}\Phi(\widehat{C}^{\mathrm{T}}\overline{X}) + u_c, \tag{31}$$

where u_c is a compensator used to reject the effect of disturbances. Here, u_c is designed as

$$u_c = -[\hat{c}_f\|\overline{X}\widehat{W}^{\mathrm{T}}\Phi'(\widehat{C}^{\mathrm{T}}\overline{X})\|_F + \hat{c}_w\|\Phi'(\widehat{C}^{\mathrm{T}}\overline{X})\widehat{C}^{\mathrm{T}}\overline{X}\| + \hat{c}_d]\mathrm{sgn}(z^{\mathrm{T}}PB). \tag{32}$$

For the weights of the RBFNN function and robustifying term, we consider the following tuning rules

$$\dot{\widehat{W}} = \Gamma_w[\Phi(\widehat{C}^{\mathrm{T}}\overline{X}) - \Phi'(\widehat{C}^{\mathrm{T}}\overline{X})\widehat{C}^{\mathrm{T}}\overline{X}]z^{\mathrm{T}}PB, \tag{33}$$

$$\dot{\widehat{C}} = \Gamma_c\overline{X}\widehat{W}^{\mathrm{T}}\Phi'(\widehat{C}^{\mathrm{T}}\overline{X})z^{\mathrm{T}}PB, \tag{34}$$

$$\dot{\hat{c}}_f = r\|\overline{X}\widehat{W}^{\mathrm{T}}\Phi'(\widehat{C}^{\mathrm{T}}\overline{X})\|_F|z^{\mathrm{T}}PB|, \tag{35}$$

$$\dot{\hat{c}}_c = r\|\Phi'(\widehat{C}^{\mathrm{T}}\overline{X})\widehat{C}^{\mathrm{T}}\overline{X}\||z^{\mathrm{T}}PB|, \tag{36}$$

$$\dot{\hat{c}}_d = r|z^{\mathrm{T}}PB|, \tag{37}$$

where Γ_w, Γ_c, and $r > 0$.

With this controller, the system (16) can be written as

$$\begin{aligned}\dot{z} &= \overline{A}z + B[W^{\mathrm{T}}\Phi(C^{\mathrm{T}}\overline{X}) - \widehat{W}^{\mathrm{T}}\Phi(\widehat{C}\overline{X})] + B(u_c + d + \epsilon)\\ &= \overline{A}z + B\Big\{\widetilde{W}^{\mathrm{T}}\Big[\Phi(\widehat{C}^{\mathrm{T}}\overline{X}) - \Phi'(\widehat{C}^{\mathrm{T}}\overline{X})\widehat{C}^{\mathrm{T}}\overline{X}\Big] + \widehat{W}^{\mathrm{T}}\Phi'(\widehat{C}^{\mathrm{T}}\overline{X})\widetilde{C}^{\mathrm{T}}\overline{X}\Big\}\\ &\quad + B(u_c + d_u + d + \epsilon).\end{aligned} \tag{38}$$

Theorem 2.1. *The plant* (16) *with controller* (31), *PID control and adaptive laws* (33)–(37), *is stable in that all the signals in the closed-loop system are bounded. In addition,* $\lim_{t\to\infty}\|z(t)\| = 0$.

Proof. Consider the following Lyapunov function candidate:

$$V = V_0 + V_1 = z^{\mathrm{T}}Pz + \widetilde{W}\Gamma_w^{-1}\widetilde{W} + \mathrm{tr}(\widetilde{C}^{\mathrm{T}}\Gamma_c^{-1}\widetilde{C}) + \frac{1}{r}[\tilde{c}_f^2 + \tilde{c}_w^2 + \tilde{c}_d^2], \tag{39}$$

where

$$V_0 = z^{\mathrm{T}}Pz, \tag{40}$$

$$V_1 = \widetilde{W}\Gamma_w^{-1}\widetilde{W} + \mathrm{tr}(\widetilde{C}^{\mathrm{T}}\Gamma_c^{-1}\widetilde{C}) + \frac{1}{r}[\tilde{c}_f^2 + \tilde{c}_w^2 + \tilde{c}_d^2]. \tag{41}$$

Taking the time derivative of V along the solution of (38), it can be shown that

$$\begin{aligned}\dot{V}_0 = {} & -z^{\mathrm{T}}z + 2z^{\mathrm{T}}PB\widetilde{W}^{\mathrm{T}}[\Phi(\widehat{C}^{\mathrm{T}}\overline{X}) - \Phi'(\widehat{C}^{\mathrm{T}}\overline{X})\widehat{C}^{\mathrm{T}}\overline{X}] \\ & + 2z^{\mathrm{T}}PB\widehat{W}^{\mathrm{T}}\Phi'(\widehat{C}^{\mathrm{T}}\overline{X})\widetilde{C}^{\mathrm{T}}\overline{X} + 2z^{\mathrm{T}}PB(u_c + d_u + d + \epsilon).\end{aligned} \tag{42}$$

Note that

$$\begin{aligned}2z^{\mathrm{T}}PB(u_c + d_u + d + \epsilon) &\leqslant 2z^{\mathrm{T}}PBu_c + 2|z^{\mathrm{T}}PB||d_u| + 2|z^{\mathrm{T}}PB|(d_M + \epsilon_M) \\ &\leqslant 2z^{\mathrm{T}}PBu_c + 2|z^{\mathrm{T}}PB|\|C\|_F\|\overline{X}\widehat{W}^{\mathrm{T}}\Phi'(\widehat{C}^{\mathrm{T}}\overline{X})\|_F \\ &\quad + 2|z^{\mathrm{T}}PB|\|W\|\|\Phi'(\widehat{C}^{\mathrm{T}}\overline{X})\widehat{C}^{\mathrm{T}}\overline{X}\| \\ &\quad + 2|z^{\mathrm{T}}PB|(d_M + \epsilon_M + 2|W|_1).\end{aligned} \tag{43}$$

Let $c_f = \|C\|_F$, $c_w = \|W\|$ and $c_d = d_M + \epsilon_M + 2|W|_1$. Then, applying the compensator u_c, we have

$$\begin{aligned}2z^{\mathrm{T}}PB(u_c + d_u + d + \epsilon) &\leqslant 2z^{\mathrm{T}}PBu_c + 2|z^{\mathrm{T}}PB|c_f\|\overline{X}\widehat{W}^{\mathrm{T}}\Phi'(\widehat{C}^{\mathrm{T}}\overline{X})\|_F \\ &\quad + 2|z^{\mathrm{T}}PB|c_w\|\Phi'(\widehat{C}^{\mathrm{T}}\overline{X})\widehat{C}^{\mathrm{T}}\overline{X}\| + 2|z^{\mathrm{T}}PB|c_d \\ &\leqslant 2|z^{\mathrm{T}}PB|(\tilde{c}_f\|\overline{X}\widehat{W}^{\mathrm{T}}\Phi'(\widehat{C}^{\mathrm{T}}\overline{X})\|_F + \tilde{c}_w\|\Phi'(\widehat{C}^{\mathrm{T}}\overline{X})\widehat{C}^{\mathrm{T}}\overline{X}\| + \tilde{c}_d) \\ &= 2[\tilde{c}_f\|\overline{X}\widehat{W}^{\mathrm{T}}\Phi'(\widehat{C}^{\mathrm{T}}\overline{X})\|_F + \hat{c}_w\|\Phi'(\widehat{C}^{\mathrm{T}}\overline{X})\widehat{C}^{\mathrm{T}}\overline{X}\| + \tilde{c}_d]|z^{\mathrm{T}}PB|.\end{aligned} \tag{44}$$

Thus,

$$\begin{aligned}\dot{V}_0 \leqslant {} & -z^{\mathrm{T}}z + 2z^{\mathrm{T}}PB\widetilde{W}^{\mathrm{T}}[\Phi(\widehat{C}^{\mathrm{T}}\overline{X}) - \Phi'(\widehat{C}^{\mathrm{T}}\overline{X})\widehat{C}^{\mathrm{T}}\overline{X}] \\ & + 2z^{\mathrm{T}}PB\widehat{W}^{\mathrm{T}}\Phi'(\widetilde{C}^{\mathrm{T}}\widetilde{X})\widetilde{C}^{\mathrm{T}}\overline{X} + 2[\tilde{c}_f\|\overline{X}\widehat{W}^{\mathrm{T}}\Phi'(\widehat{C}^{\mathrm{T}}\overline{X})\|_F \\ & + \tilde{c}_w\|\Phi'(\widehat{C}^{\mathrm{T}}\overline{X})\widehat{C}^{\mathrm{T}}\overline{X}\| + \tilde{c}_d]|z^{\mathrm{T}}PB|.\end{aligned} \tag{45}$$

Note that $z^{\mathrm{T}}PB$ is a scalar. For $\dot{V}$, we have

$$\begin{aligned}
\dot{V} \leqslant & -\|z\|^2 - 2\widetilde{W}^{\mathrm{T}}\Gamma_w^{-1}\dot{\widehat{W}} + 2\widetilde{W}^{\mathrm{T}}[\Phi(\widehat{C}^{\mathrm{T}}\overline{X}) - \Phi'(\widehat{C}^{\mathrm{T}}\overline{X})\widehat{C}^{\mathrm{T}}\overline{X}]z^{\mathrm{T}}PB \\
& - 2\mathrm{tr}(\widetilde{C}^{\mathrm{T}}\Gamma_c^{-1}\dot{\widehat{C}}) + 2\widehat{W}^{\mathrm{T}}\Phi'(\widehat{C}^{\mathrm{T}}\overline{X})\widetilde{C}^{\mathrm{T}}\overline{X}_z^{\mathrm{T}}PB \\
& - \frac{2}{r}\tilde{c}_f\dot{\tilde{c}}_f + 2\tilde{c}_f\|\overline{X}\widehat{W}^{\mathrm{T}}\Phi'(\widehat{C}^{\mathrm{T}}\overline{X})\|_F|z^{\mathrm{T}}PB| - \frac{1}{r}2\tilde{c}_w\dot{\tilde{c}}_w \\
& + 2\tilde{c}_w\|\Phi'(\widehat{C}^{\mathrm{T}}\overline{X})\widehat{C}^{\mathrm{T}}\overline{X}\||z^{\mathrm{T}}PB| - \frac{2}{r}\tilde{c}_d\dot{\tilde{c}}_d + \tilde{c}_d|z^{\mathrm{T}}PB| \\
\leqslant & -\|z\|^2 + 2\{-\widetilde{W}^{\mathrm{T}}\Gamma_w^{-1}\dot{\widehat{W}} + [\Phi(\widehat{C}^{\mathrm{T}}\overline{X}) - \Phi'(\widehat{C}^{\mathrm{T}}\overline{X})\widehat{C}^{\mathrm{T}}\overline{X}]z^{\mathrm{T}}PB\} \\
& + 2tr\widetilde{C}^{\mathrm{T}}[-\Gamma_c^{-1}\dot{\widehat{C}} + \overline{X}\widehat{W}^{\mathrm{T}}\Phi'(\widehat{C}^{\mathrm{T}}\overline{X})z^{\mathrm{T}}PB] \\
& + 2\tilde{c}_f\left[-\frac{1}{r}\dot{\tilde{c}}_f + \|\overline{X}\widehat{W}^{\mathrm{T}}\Phi'(\widehat{C}^{\mathrm{T}}\overline{X})\|_F|z^{\mathrm{T}}PB|\right] \\
& + 2\tilde{c}_w\left[-\frac{1}{r}\dot{\tilde{c}}_w + \|\Phi'(\widehat{C}^{\mathrm{T}}\overline{X})\widehat{C}^{\mathrm{T}}\overline{X}\||z^{\mathrm{T}}PB|\right] \\
& + 2\tilde{c}_d\left[-\frac{1}{r}\dot{\tilde{c}}_d + |z^{\mathrm{T}}PB|\right]. \qquad (46)
\end{aligned}$$

Substituting the RBFNN weights' and parameters' update laws (33)–(36) into (46) yields

$$\dot{V} \leqslant -\|z\|^2. \qquad (47)$$

This implies that all the signals of the closed-loop system are uniformly bounded.

From (38) and the fact that $\overline{X}$, Φ, ϵ, d are bounded and the system parameters are bounded, it follows that $\|\dot{z}\|_2$ is bounded. Eq. (47) and the definiteness of V imply that

$$\int_0^\infty \|z\|^2 \mathrm{d}t \leqslant \int_0^\infty -\dot{V}(\tau)\mathrm{d}\tau + \mathrm{const.} \qquad (48)$$

This implies that $\|z\|_2 \in L_2$. Applying Barbalat's lemma, we obtain

$$\lim_{t\to\infty}\|z\|_2 = 0. \qquad (49)$$

The proof is completed. □

Remark 2.1. The RBFNN reconstruction error ϵ is a critical quality to meet Theorem 2.1, representing the minimum possible deviation between the unknown function $f(x,\dot{x})$ and the function estimation $\hat{f}(x,\dot{x})$. In general, increasing the RBFNN node number reduces the RBF reconstruction error.

Remark 2.2. The proposed controller differs from the controller of Lewis et al. [14] and Zhang et al. [15]. Our controller can achieve an error approaching zero, while their controllers can achieve the error approaching to a small region.

Theorem 2.1 relates only to the asymptotic performance requirement in the closed-loop system, no transient performance is discussed. In practical applications,

transient performance can be even more important. To this end, we have the following theorem.

Theorem 2.2. *For the closed-loop system* (38), *then the tracking error bound on the* L_2 *norm is*

$$\|z\|_2 \leqslant \sqrt{\lambda_{\max}(P)}\|z(0)\| + \frac{1}{\sqrt{\lambda_{\min}(\Gamma_w)}}\|\widetilde{W}(0)\| + \frac{1}{\sqrt{\lambda_{\min}(\Gamma_c)}}\|\widetilde{C}(0)\| + \frac{1}{\sqrt{r}}(|\tilde{c}_f(0)| + |\tilde{c}_w(0)| + |\tilde{c}_d(0)|). \tag{50}$$

Proof. From (47), we have

$$\dot{V} \leqslant -\|z\|^2. \tag{51}$$

It follows that

$$\|z\|^2 \leqslant -\dot{V}. \tag{52}$$

Since $V = z^{\mathrm{T}}Pz + \widetilde{W}\Gamma_w^{-1}\widetilde{W} + \widetilde{C}^{\mathrm{T}}\Gamma_c^{-1}\widetilde{C} + \frac{1}{r}[\tilde{c}_f^2 + \tilde{c}_w^2 + \tilde{c}_d^2]$ is nonincreasing and bounded from below by zero, it will be limited as $t \to \infty$, so that

$$\begin{aligned}\|z\|^2 &= \int_0^\infty \|z(\tau)\|^2 \,\mathrm{d}\tau \leqslant -\int_0^\infty \dot{V}(\tau)\,\mathrm{d}\tau = V(0) - V(\infty) \leqslant V(0)\\ &= z^{\mathrm{T}}(0)Pz(0) + \widetilde{W}(0)\Gamma_w^{-1}\widetilde{W}(0) + \widetilde{C}^{\mathrm{T}}(0)\Gamma_c^{-1}\widetilde{C}(0) + \frac{1}{r}[\tilde{c}_f(0)^2 + \tilde{c}_w(0)^2 + \tilde{c}_d(0)^2]\\ &\leqslant \lambda_{\max}(P)\|z(0)\|^2 + \frac{1}{\lambda_{\min}(\Gamma_w)}\|\widetilde{W}(0)\|^2 + \frac{1}{\lambda_{\min}(\Gamma_c)}\|\widetilde{C}(0)\|^2 + \frac{1}{r}[\tilde{c}_f(0)^2 + \tilde{c}_w(0)^2 + \tilde{c}_d(0)^2],\end{aligned} \tag{53}$$

which implies (50). □

Remark 2.3. Theorem 2.2 provides some methods for improving the transient performance. (1) The nonzero initial parameter error of $W_i^* - W_i(0)$ may increase the error bound. However, with a NN trained off-line, we can reduce the initial error. (2) Large adaptation gains Γ_w, Γ_c, r which attenuate the effects of initial parameter error is vital for good L_2 performance.

3. Simulation and experimental study

In this section, a simulation study is provided to demonstrate the performance of the proposed algorithms on mechanical systems. A piezoelectric linear motor (Fig. 3) manufactured by Nanomotion is used as the test platform for our purpose. The linear motor is mounted on a single axis linear stage manufactured by Steinmeyer.

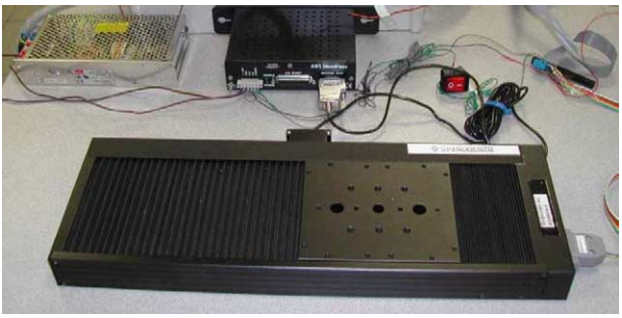

Fig. 3. Test platform: piezoelectric linear motor.

Table 1
Specification of piezoelectric linear motor

Travel	Velocity (max)	Resolution	Output force (max)
200 mm	250 mm/s	0.1 μm	40 N

Table 1 shows the specifications of the stage and the motor. The motor is modeled as a nonlinear differential equation as given in (4), with $K_f = 8$ N/V, $K_e = 144$ N s/m, $M = 5.3$ kg, and $R = 1.5\ \Omega$.

The nominal plant model (ignoring frictional force f_{fric} in (10)) in (4) may also be expressed as

$$G_p(s) = \frac{k_p}{s(T_p s + 1)}, \tag{54}$$

where k_p, T_p are the model parameters.

The nominal model of the plant is first identified off-line using a relay feedback method [13]. The model parameters in (54) are identified as $k_p = 4.3823\text{e}5$, $T_p = 0.009$. Using the dual relay feedback method [17,18], the friction parameters in (10) are identified as $f_1 = 0.0064$, $f_2 = 8.2876\text{e}{-5}$ and $\delta f = 0.381$. Using these system parameters, a PID feedback controller can be commissioned. The controller can be designed based on a wide range of well-developed PID tuning methodologies [13]. The desired displacement trajectory is shown in Fig. 4. A main consideration of the trajectory selected is that it has to be first-order integrable and differentiable. One of the strengths of the proposed method is that only a stable set of PID parameters (which can be easily obtained using the nominal plant model) is required. In the simulation example, only one or two relay experiments are performed to obtain the PID parameters.

For simulation purposes, three cases (i.e., *Case 1*: PID controller on the nominal plant (without considering the frictional force); *Case 2*: PID controller on the full nonlinear plant; *Case 3*: Combined PID/adaptive controller on the full nonlinear plant) are considered. The simulation results of the tracking performance in all three

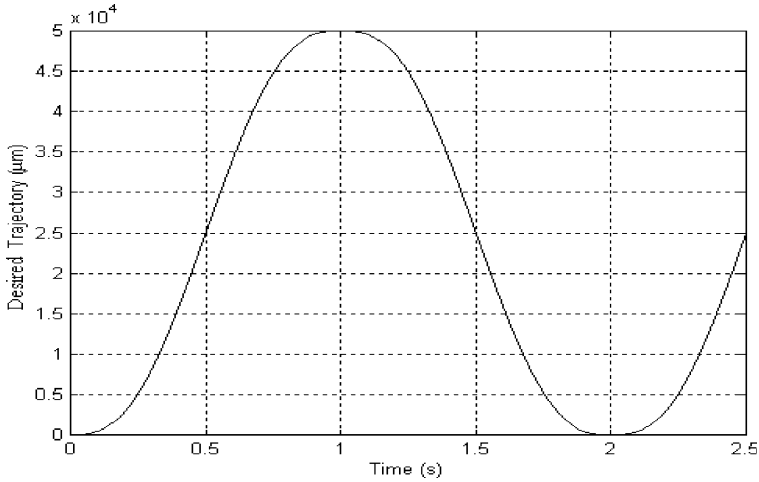

Fig. 4. Desired trajectory.

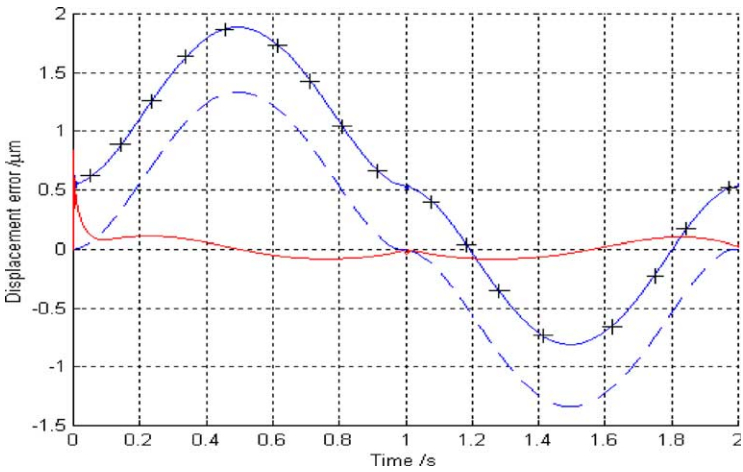

Fig. 5. Comparison of the displacement error in all three cases. (dash line) Case 1: PID controller on the nominal plant; (+) Case 2: PID controller on the full nonlinear system; (full line) Case 3: combined PID/adaptive controller on the full nonlinear system.

cases are shown in Fig. 5. For the adaptive controller, 40 nodes are used in the RBFNN. As seen in Fig. 5, the combined PID and adaptive controller exhibits good learning capabilities and convergence properties while performing the tracking tasks. The displacement error is much reduced when the adaptive controller is commissioned in the full nonlinear system. The effect of including the frictional force in the simulation model is evident in that the displacement error is increased, as compared

to the case with just the nominal plant. The PID controller alone is not adequate for the motion tracking purposes. The adaptive controller provides the major portion of the control action.

An actual experimental study is conducted on the actual piezoelectric platform. The same desired displacement trajectory as shown in Fig. 4 is used in this experimental study. The tracking performance of the PID controller alone is shown in Fig. 6. With the additional adaptive controller applied to the full nonlinear system, the tracking performance of the combined PID and adaptive controller is shown in Fig. 7.

As the desired trajectory is repetitive in nature, the forward and backward linear motion of the moveable translator along the motor stage is shown in Figs. 6 and 7. With PID controller alone, the amplitude of the displacement error remains fairly constant at about 120 μm. There is just a change of sign in the displacement error as the translator moves from the forward motion and back. It can be observed that there is a step-like increase in the displacement error as the translator changes its direction of motion. This is due largely to the frictional forces [10], which includes viscous and Coulomb friction, at work. Combining the efforts of the RBFNN and PID controller, the displacement error (Fig. 7) is greatly reduced. There is an initial spike-like increase in the displacement error as the translator changes its direction of motion. But the RBFNN is able to clamp down on the displacement error for the rest of the motion, until the translator changes its direction of motion again. For the

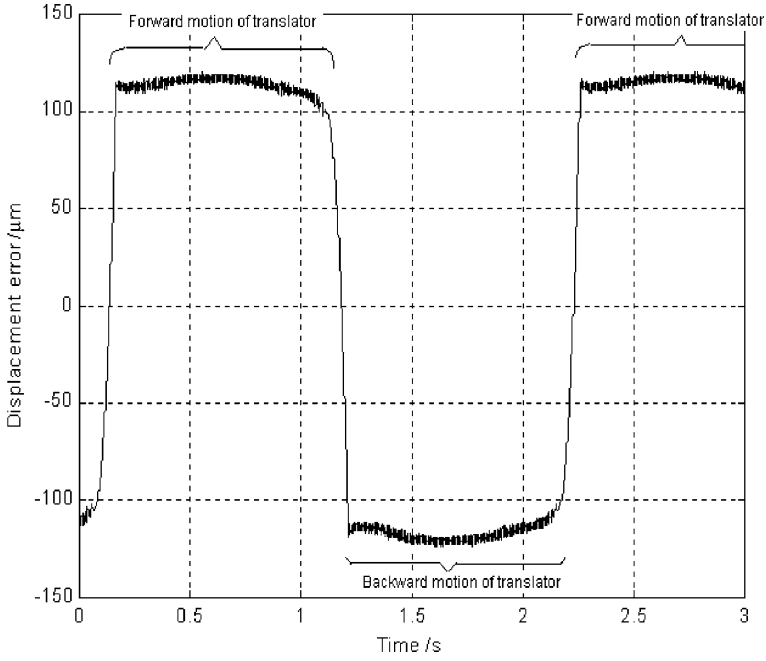

Fig. 6. Tracking performance of the PID controller on the actual piezoelectric motor.

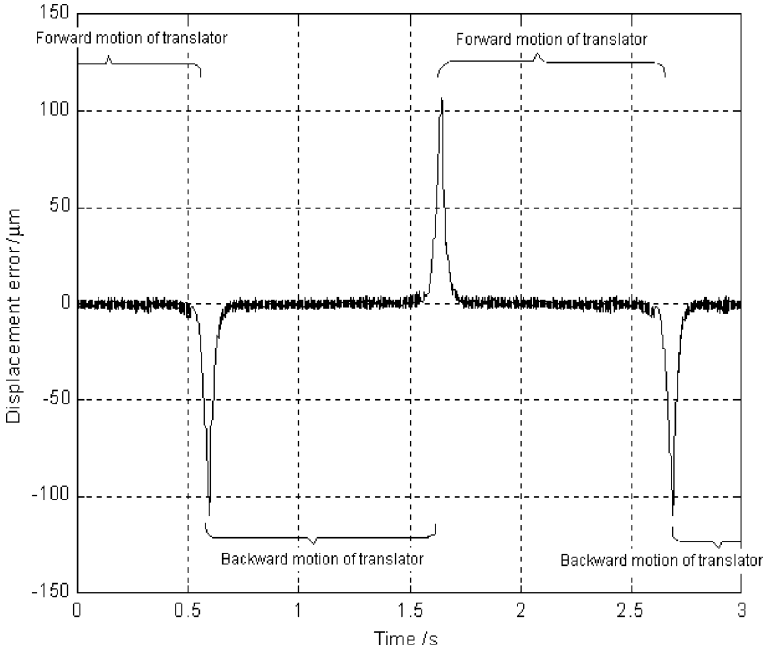

Fig. 7. Tracking performance of the combined PID/adaptive controller on the actual piezoelectric motor.

adaptive controller, 30 nodes are used in the RBFNN in this experimental study. The results of the experimental study is consistent with that of the simulation study. The combined PID and adaptive controller achieves good tracking performance, in the face of strong nonlinearities in the system.

4. Conclusions

This paper has considered the development of a new PID/adaptive controller for a class of nonlinear systems. The second-order model is used as the nominal dominant model for the design of the PID controller, and an adaptive component designed based on a RBFNN provides for the possibility of performance enhancement when the feedback control alone is inadequate to cope with uncertain nonlinear phases. The effectiveness of the proposed control scheme is highlighted in the simulation and experimental study.

References

[1] Hang CC, Astrom KJ, Ho WK. Refinements of the Ziegler–Nichols tuning formula. IEE Proc Part D 1991;138(2):111–8.
[2] Astrom KJ, Hagglund T. Automatic tuning of PID controllers. Research Triangle Park, USA: Instrument Society of America; 1988.

[3] Shinskey FG. Process control system: application, design and tuning. 3rd ed. New York: McGraw-Hill; 1988.
[4] Rivera DE, Morari M, Skogestad S. Internal model control for PID controller design. Ind Eng Chem Process Des Dev 1986;25:252–65.
[5] Huang HP, Chen CL, Lai CW, Wang GB. Auto-tuning for model based PID controllers. AIChE J 1996;42(9):2687–91.
[6] Xu Y, Hollerbach JM, Ma D. A nonlinear PD controller for force and contact transient control. IEEE Control Syst 1995;15(1):15–21.
[7] Huang SN, Tan KK, Lee TH. Further results on adaptive control for a class of nonlinear systems using neural networks. IEEE Transactions on Neural Networks 2003;14(3):719–22.
[8] Tan KK, Lim SY, Huang SN. Two-degree-of-freedom controller incorporating RBF adaptation for precision motion control applications. In: IEEE/ASME International Conference on Advanced Intelligent Mechatronics (AIM' 99), Atlanta, USA, 1999. p. 848–53.
[9] Fujimoto Y, Kawamura A. Robust servo-system based on two-degree-of-freedom control with sliding mode. IEEE Trans Ind Electron 1995;42(3):272–80.
[10] Armstrong-Helouvry B, Dupont P, de Wit CC. A survey of models, analysis tools and compensation methods for the control of machines with friction. Automatica 1994;30(7):1083–138.
[11] Hornik K, Stinchcombe M, White H. Multilayer feedforward networks are universal approximators. Neural Networks 1989;2:359–66.
[12] Fabri S, Kadirkamanathan V. Dynamic structure neural networks for stable adaptive control of nonlinear systems. IEEE Trans Neural Networks 1996;7(5):1151–67.
[13] Tan KK, Wang QG, Hang CC, Hagglund T. Advances in PID control. London: Springer-Verlag London Limited; 1999.
[14] Lewis FL, Yesildirek A, Liu K. Multilayer neural-net robot controller with guaranteed tracking performance. IEEE Trans Neural Networks 1996;7(2):388–98.
[15] Zhang T, Ge SS, Hang CC. Design and performance analysis of a direct adaptive controller for nonlinear systems. Automatica 1999;35:1809–17.
[16] Astrom KJ, Hagglund T. PID controllers: theory, design and tuning. 2nd ed. Research Triangle Park, USA: Instrument Society of America; 1995.
[17] Tan KK, Lee TH, Dou HF, Huang SN. Precision motion control. London: Springer-Verlag London Limited; 2001.
[18] Friman M, Waller KV. A two-channel relay for autotuning. Ind Eng Chem Res 1997;36:2662–71.